Sensors and Actuators B 182 (2013) 71–79

Contents lists available at SciVerse ScienceDirect

Sensors and Actuators B: Chemical

journal homepage: www.elsevier.com/locate/snb

Chaotic time series prediction of E-nose sensor drift in embedded phase space

Lei Zhang[a,*], Fengchun Tian[a], Shouqiong Liu[b], Lijun Dang[a], Xiongwei Peng[a], Xin Yin[a]

[a] College of Communication Engineering, Chongqing University, 174 ShaZheng Street, ShaPingBa District, Chongqing 400044, China
[b] Academy of Metrology and Quality Inspection, Chongqing 401123, China

ARTICLE INFO

Article history:
Received 8 November 2012
Received in revised form 28 February 2013
Accepted 1 March 2013
Available online xxx

Keywords:
Sensor drift
Chaotic time series
Long-term prediction
Phase space reconstruction
Radial basis function neural network

ABSTRACT

Chemical sensor drift shows a chaotic behavior and unpredictability in long-term observation which makes it difficult to construct an appropriate sensor drift treatment. The main purpose of this paper is to study a new methodology for chaotic time series modeling of chemical sensor observations in embedded phase space. This method realizes a long-term prediction of sensor baseline and drift based on phase space reconstruction (PSR) and radial basis function (RBF) neural network. PSR can memory all of the properties of a chaotic attractor and clearly show the motion trace of a time series, thus PSR makes the long-term drift prediction using RBF neural network possible. Experimental observation data of three metal oxide semiconductor sensors in a year demonstrate the obvious chaotic behavior through the Lyapunov exponents. Results demonstrate that the proposed model can make long-term and accurate prediction of chemical sensor baseline and drift time series.

1. Introduction

Artificial olfaction system such as electronic nose (E-nose) is becoming a very promising method to monitor air contaminates in environmental field. Chemical sensors have been widely used for the analysis of volatile organic compounds. An E-nose is an instrument which employs a sensor array of chemical sensors but only semi-selective gas sensors with pattern recognition, and provides a higher degree of selectivity and reversibility leading to an extensive range of applications [1,2]. However, sensors are often operated over a long period time in real-world application, and aging will reduce the lifetime of sensors. Sensor drift is caused by unknown dynamic process in the sensor system including poisoning, aging of sensors or environmental variations [3]. The drift will decrease the selectivity and sensitivity of sensors, and an E-nose consisting of drifting sensors will lose its effectiveness as a usable monitor because the previous pattern recognition model cannot fit the drifted array space. Therefore, the sensor drift with gradual and unpredictable variation of sensor response has been recognized as the most challenging issue in E-nose development [4].

In recent years, many drift counteraction methods have been proposed by researchers. The most commonly used methods are multivariate component correction [5], principal component analysis [6,7], adaptive drift correction based on evolutionary algorithm [8], orthogonal signal correction [9], and drift compensation based on estimation theory [10]. However, all the methods assume that the long-term sensor drift trend can be tracked through the drift direction in principal component space or the samples' distribution. Unfortunately, the long-term sensor drift has no regular trend and the sensor drift is not always positive or negative from a long-term view [4]. In addition, previous methods can only be analyzed off-line in computer, and it is difficult to be used in real-life application. Therefore, through a long-term observation of sensor response within one year, we studied the chaotic characteristic of long-term sensor response using Lyapunov exponents in embedded phase space, and proposed a novel drift prediction model using chaotic time series prediction method based on phase space reconstruction and RBF neural network.

Chaos is a universal phenomenon of nonlinear dynamic systems. Chaos is an irregular motion, and seemingly unpredictable random behavior exhibited by a deterministic nonlinear system under deterministic conditions. Chaotic time series prediction is based on Phase Space Reconstruction (PSR), and aims to find the embedding way, dimensions and time delay of attractor in terms of the present observation sequence [11,12]. The time series will reconstruct the attractor of system in a high dimension without changing its topology, an appropriate time delay will transform the prediction problem into a short evolutionary process in phase space. Phase space reconstruction reserves the attractor's properties. Therefore, to an unknown drift model, application of chaotic attractor theory for drift prediction in embedded phase space is reasonable.

* Corresponding author. Tel.: +86 13629788369; fax: +86 23 65111745.
E-mail address: leizhang@cqu.edu.cn (L. Zhang).

0925-4005/$ – see front matter © 2013 Elsevier B.V. All rights reserved.
http://dx.doi.org/10.1016/j.snb.2013.03.003

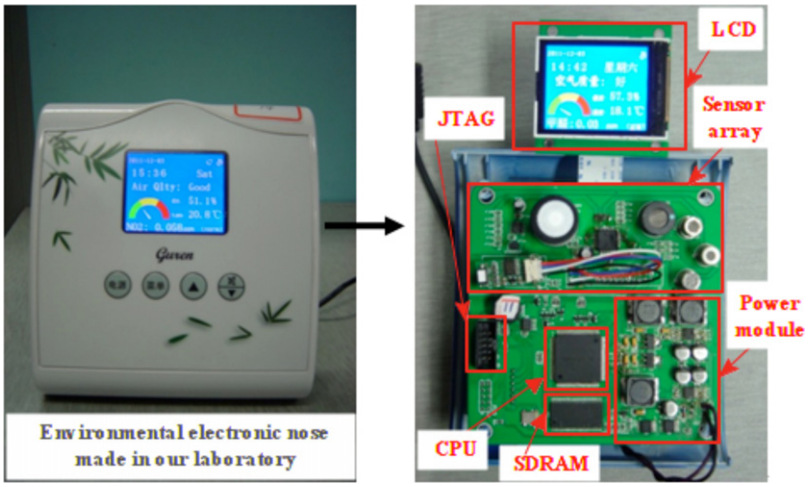

Fig. 1. Self-designed electronic nose for indoor air quality monitoring. The left picture is the integral electronic nose; the right picture is the internal PCB with integrated circuits with the main modules labeled.

2. Data

2.1. Long-term sensor baseline data

In our previous publications [13–15], our electronic nose system has been presented. The picture of our electronic nose made in our laboratory and the internal circuit of PCB (print circuit board) has been illustrated in Fig. 1. The JTAG (Joint Test Action Group) is used for communication between PC and the PCB, such as write programs from PC to the CPU, and read data from the CPU to PC. Three metal oxide semiconductor sensors were studied in this work for sensor drift. They are TGS2620 and TGS2201 with dual outputs (TGS2201A/B). The sensors started work on September 04, 2011, and stopped on July 06, 2012. The operation surrounding of sensors is inside the room. The heater voltage is 5 V. The total number of sampling points for each sample is set as 3000. Therefore, we read the data from the instrument for about 3 days. Totally, 136 samples were obtained in order within one year. Consider that the redundancy of 3000 sampling points in each sample around 3 days will cause the complexity of analysis, thus, we extract 100 points uniformly from each sample with the interval of 30 points. Totally, 13,600 points of sensor baseline within one year were obtained. Fig. 2 illustrates the extracted observations of each sensor within one year. We can find from Fig. 2 that there is a reduction of sensor response at the approximated position of 6725. It is due to that the temperature indoor descends when the air conditioner was turned on, and results in a reduction of sensor response. Note that the unit of sensors' raw outputs is voltage (V), however, the responses in Fig. 2 is the output of 12 bit-ADC (analogy to digital converter) after 0–1 normalization by dividing the maximum 4095 (2^{12}–1).

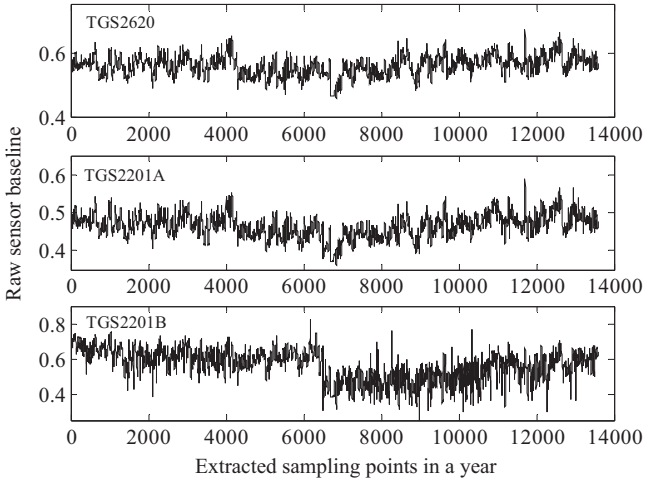

Fig. 2. Raw observation points of sensors.

2.2. Long-term drift extraction using discrete fourier transform (DFT)

Although sensor drift is difficult to describe, some properties of drift are known. The drift has a low-frequency behavior, and it can also be considered as a band-limited signal [16]. The sensor baseline is extremely related with environmental factors (e.g. temperature, humidity and pressure). Therefore, DFT is used for spectrum analysis of the long-term sensor signal. The representation of DFT is shown as

$$X(k) = \frac{1}{N}\sum_{n=0}^{N-1} x(n)e^{-j\cdot(2\pi/N)\cdot k\cdot n}, \quad k = 0, \quad 1, \ldots, N-1 \tag{1}$$

where $\{x(n), n = 0,\ldots, N-1\}$ denotes the sensor baseline signal vector, N is the length of vector x, and $\{X(k), k = 0,\ldots, N-1\}$ denotes the DFT.

Fig. 3 presents the spectrum plots (real part) of three sensors through the DFT operation. In this work, the frequency segment between 0.0001 and 0.001 Hz are selected as desired spectrum of drift signal, and the spectrum is set to 0 for other frequencies. Generally, the frequency components of environmental factors should be lower than drift. Then, an inverse DFT (IDFT) is employed for drift signal in time domain. The representation of IDFT is shown as

$$\tilde{x}(n) = \sum_{k=0}^{N-1} X(k)e^{j\cdot(2\pi/N)\cdot k\cdot n}, \quad n = 0, \quad 1, \ldots, N-1 \tag{2}$$

where $\{\tilde{x}(n), \quad n = 0, \ldots, N-1\}$ denotes the reconstructed drift signal in time domain.

Fig. 4 presents the reconstructed drift signal of three sensors using IDFT operations.

It is worthy noting that this work is realized with two potential assumptions: first, the sensor drift shows a sufficiently low frequency; second, the drift from the long-term data time series should not change during the practical lifetime of the E-nose.

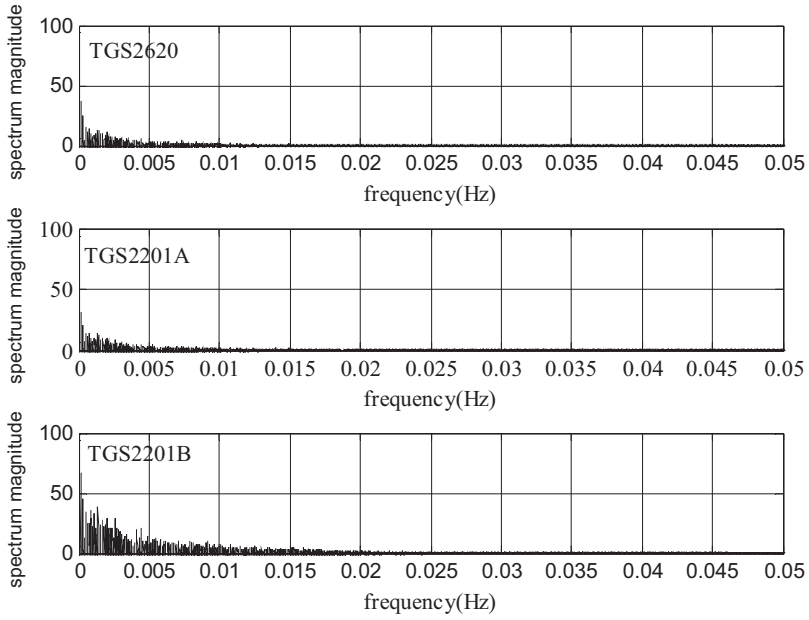

Fig. 3. Spectrum plots of DFT for three sensors.

3. Chaotic time series prediction

3.1. Phase space reconstruction

Phase space reconstruction (PSR) is the basic theory in analysis of chaotic dynamic systems, founded by Taken [17]. Taken's theorem proves that we can reconstruct a phase space from a one-dimension chaotic time series which has an equal phase space with dynamic system in topology. The discrimination, analysis and prediction are employed in the reconstructed phase space, thus PSR is the key point in chaotic time series study. The embedding dimension m and time delay τ are the most important variables in PSR. The selections of m and τ have been well studied by researchers in chaos [18–23]. In this paper, False Nearest Neighbors (FNN) method [18] is used to determine the embedding dimension m. Auto-correlated function is used to calculate the time delay τ [18,19].

Given a chaotic time series $\{x(n), n = 1,\ldots,N\}$, the reconstructed phase space can be represented by

$$X(t) = \{x(t),\ x(t+\tau),\ \ldots,\quad x(t+(m-1)\cdot\tau)\} \tag{3}$$

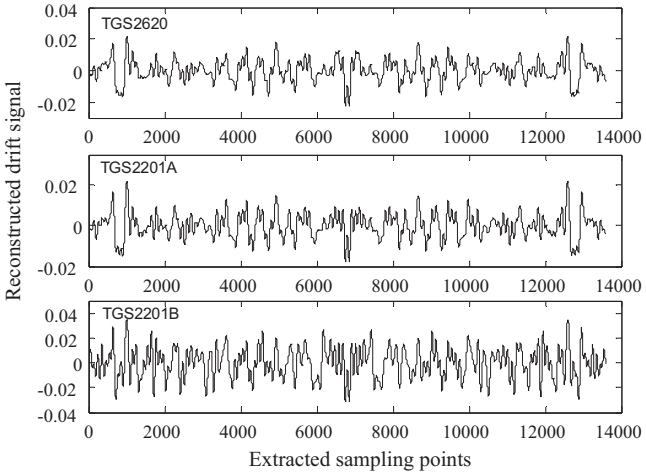

Fig. 4. Reconstructed sensor drift signal using IDFT.

where $t = 1,\ldots,N-(m-1)\tau-1$, and m ($m = 2,3,\ldots$) is the embedding dimension, provided that $m \geq 2D+1$, and D is the fractal dimension of attractor.

For clarity, we expand the formula (3) as follows

$$\begin{cases} X(1) = [x(1),\quad x(1+\tau),\ldots,x(1+(m-1)\cdot\tau)]^T \\ X(2) = [x(2),\quad x(2+\tau),\ldots,x(2+(m-1)\cdot\tau)]^T \\ X(3) = [x(3),\quad x(3+\tau),\ldots,x(3+(m-1)\cdot\tau)]^T \\ \ldots \\ X(N-(m-1)\cdot\tau-1) = [x(N-(m-1)\cdot\tau-1), x(N-(m-2)\cdot\tau),\ldots,x(N-1)]^T \end{cases} \tag{4}$$

where symbol T denotes the transpose of a vector.

Lyapunov exponent is a useful tool to characterize a chaotic attractor quantitatively, which effectively measures the sensitivity of the chaotic orbit to its initial conditions and quantizes the attractor's dynamics of a complex system. When the Lyapunov exponent λ of a time series is positive, then the time series will become chaotic [12]. The computation of Lyapunov exponent in this work is employed using classical Wolf-method [24].

For example of PSR analysis, we generate a time series by numerically integrating the Lorenz system which consists of three ordinary differential equations [25]. The representation of Lorenz system is shown as

$$\begin{cases} \dfrac{dx}{dt} = \sigma\cdot(y-x) \\ \dfrac{dy}{dt} = r\cdot x - y - x\cdot z \\ \dfrac{dz}{dt} = -b\cdot z + x\cdot y \end{cases} \tag{5}$$

where x is proportional to the intensity of convective motion; y is proportional to the horizontal temperature variation; z is proportional to the vertical temperature variation; σ, r and b are constants. For analysis, the parameters σ, r, and b are set as 25, 3 and 50, respectively; the step size of integration is set to 0.01; the initial value of y is $[-1, 0, 1]^T$. Fig. 5 illustrates the PSR of Lorenz attractor in which the embedding dimension $m = 3$ and time delay $\tau = 1$.

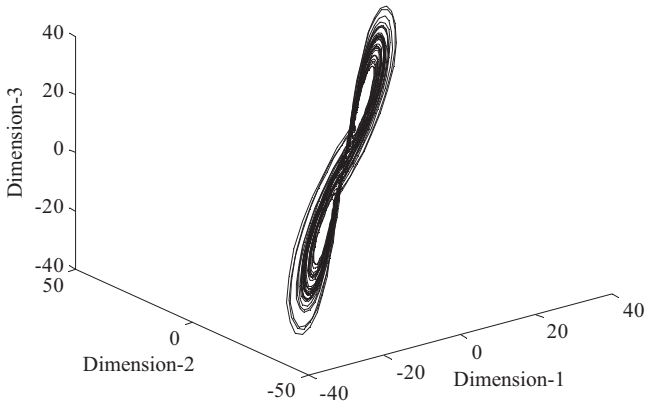

Fig. 5. Three dimensional PSR of Lorenz attractor.

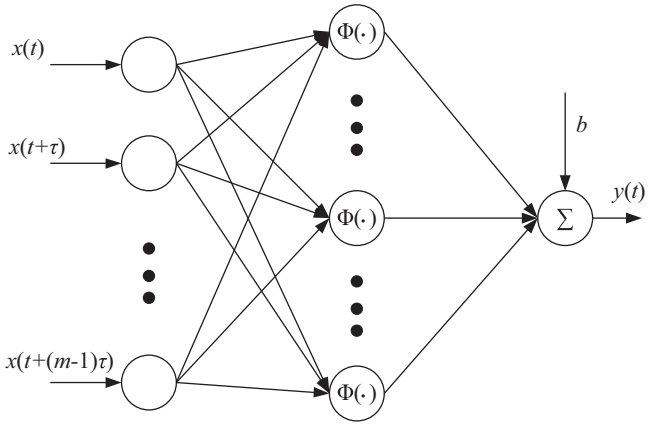

Fig. 6. Structure of RBF neural network for prediction in PSR.

3.2. Prediction model

In chaotic time series prediction, RBF (radial basis function) neural network is used to trace the attractor in embedded phase space for each sensor. The use of RBF to model strange attractors representing time series data has been referred in [26]. RBF neural network [27] is a forward feedback artificial neural network composed of three layers. The number of input nodes depends on the embedding dimension m. The input signal is just the reconstructed $X(t)$ ($t = 1,\ldots, N-(m-1)\tau$) in phase space. In the hidden layer, a Gaussian function is used as activation function. The structure of RBF neural network prediction in PSR is shown as Fig. 6.

Combined with Eq. (4), the training input matrix can be shown by

$$P = [X(1), X(2), \ldots, X(N-(m-1)\cdot\tau-1)] \quad (6)$$

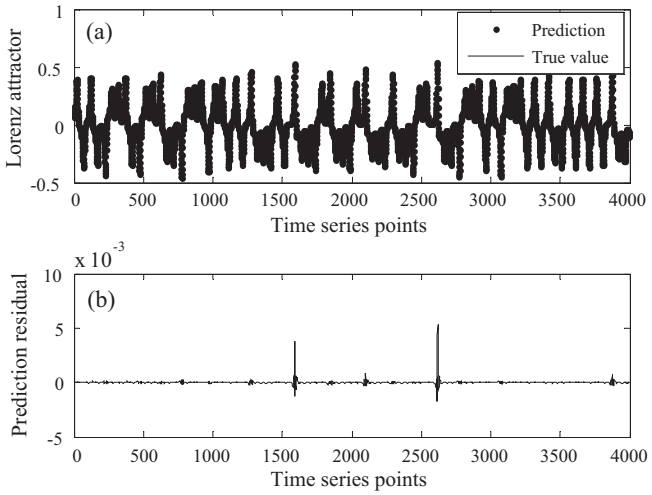

Fig. 7. Prediction of Lorenz time series using the proposed model.

After expansion of P using formula (4) and (6), we obtain

$$P = \begin{bmatrix} x(1) & x(2) & \cdots & x(N-(m-1)\cdot\tau-1) \\ x(1+\tau) & x(2+\tau) & \cdots & x(N-(m-2)\cdot\tau-1) \\ \vdots & \vdots & \vdots & \vdots \\ x(1+(m-1)\cdot\tau) & x(2+(m-1)\cdot\tau) & \cdots & x(N-1) \end{bmatrix} \quad (7)$$

Then the vector of training goal is represented as

$$T = [x(2+(m-1)\cdot\tau), x(3+(m-1)\cdot\tau), \cdots, x(N)] \quad (8)$$

In this paper, three models are constructed for TGS2620, TGS2201A and TGS2201B, respectively. The chaotic time series prediction can be concluded as two steps: Phase space reconstruction and RBF neural network learning. We apply the method to Lorenz attractor prediction for example analysis. We select 5000 points in Lorenz sequence for prediction, in which the first 1000 points are used for RBF neural network learning and the remaining 4000 points as test. The test results are presented in Fig. 7(a) and (b), which illustrate the prediction of Lorenz chaotic time series and the prediction residual error, respectively. We can see in Fig. 7 that the prediction of Lorenz chaotic time series is successful using the proposed model.

The well known statistics RMSEP (root mean square error of prediction) [28] is also used to quantitatively measure the sensor baseline and drift prediction models in this work. Its representation can be expressed as

$$\mathrm{RMSEP} = \sqrt{\frac{1}{N-1}\cdot\sum_{t=1}^{N}\left[s(t)-\hat{s}(t)\right]^2} \quad (9)$$

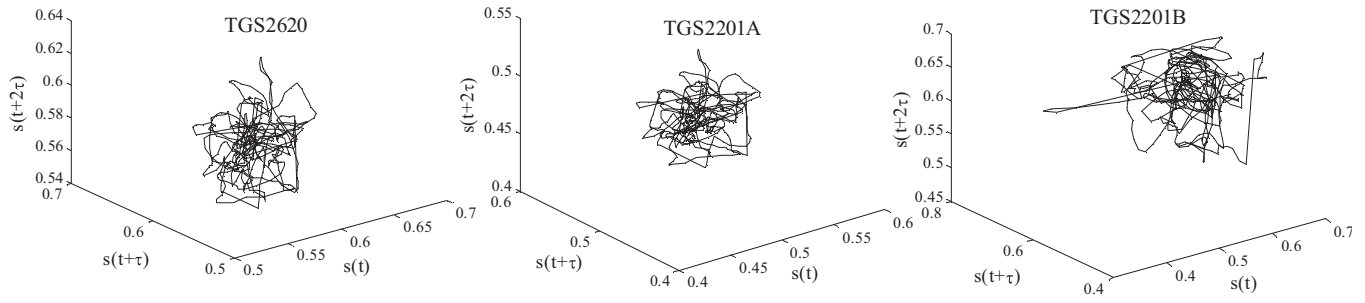

Fig. 8. PSR plots of long-term sensor observation data.

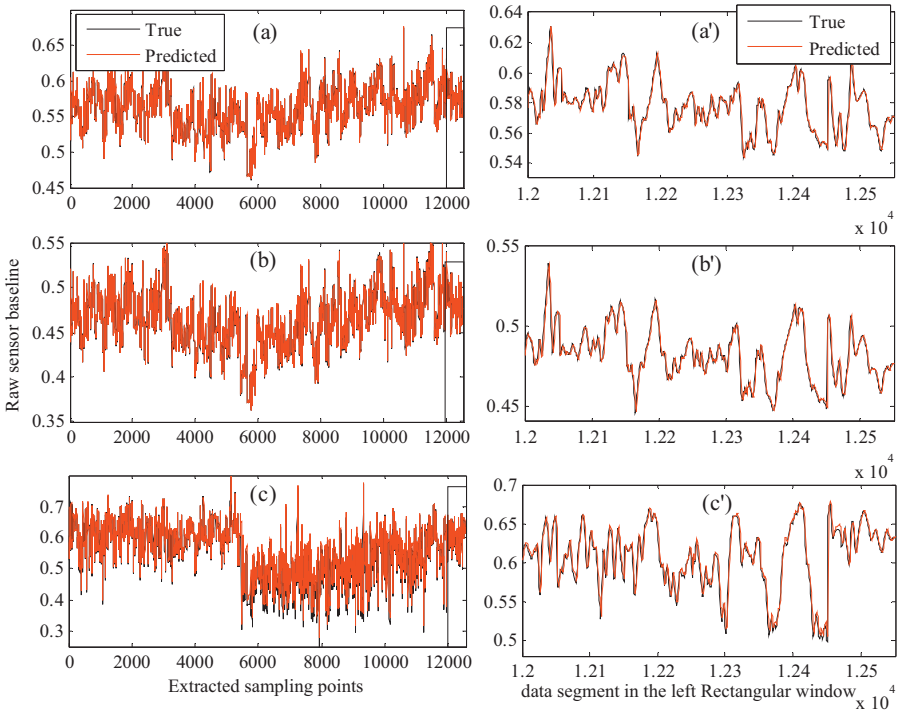

Fig. 9. Predictions of long-term sensor baseline using the proposed model.

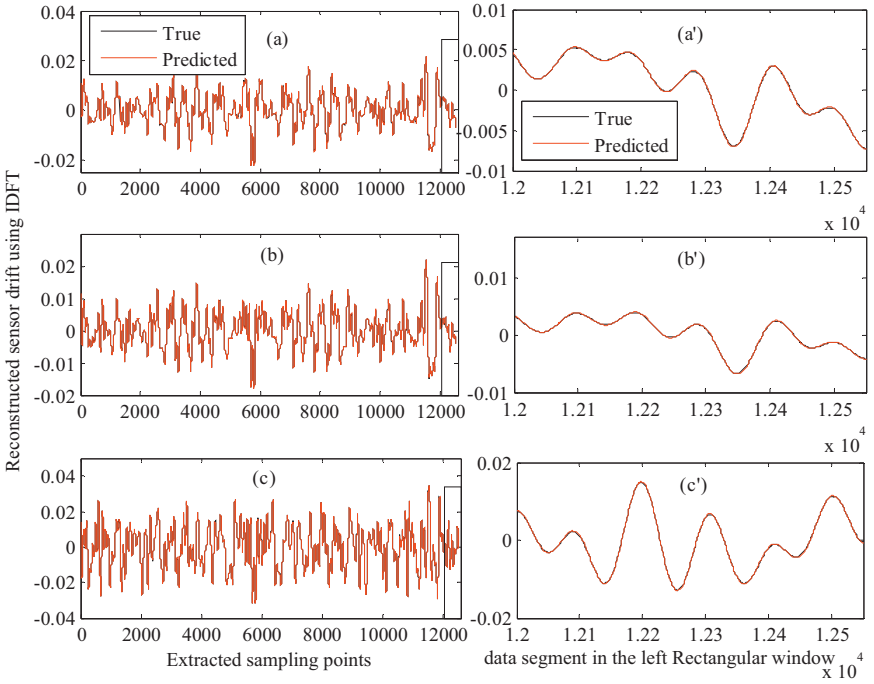

Fig. 10. Predictions of reconstructed sensor drift signal using the proposed model.

Table 1
RMSEP of sensor baseline and drift prediction modeling with different Ntr of training data points.

Ntr	RMSEP of sensor baseline prediction			RMSEP of sensor drift prediction		
	TGS2620	TGS2201A	TGS2201B	TGS2620	TGS2201A	TGS2201B
100	0.0319	0.0330	0.5719	4.64e−04	5.44e−04	4.49e−04
250	0.0102	0.0121	0.0684	5.33e−04	3.72e−04	5.92e−04
500	0.0054	0.0060	0.0290	1.05e−04	9.09e−05	3.02e−04
750	0.0045	0.0044	0.0170	7.28e−05	6.71e−05	1.58e−04
1000	0.0045	0.0044	0.0179	5.69e−05	5.25e−05	1.13e−04
1250	0.0046	0.0045	0.0288	5.37e−05	4.93e−05	1.15e−04
1500	0.0046	0.0045	0.0177	5.31e−05	4.87e−05	1.16e−04

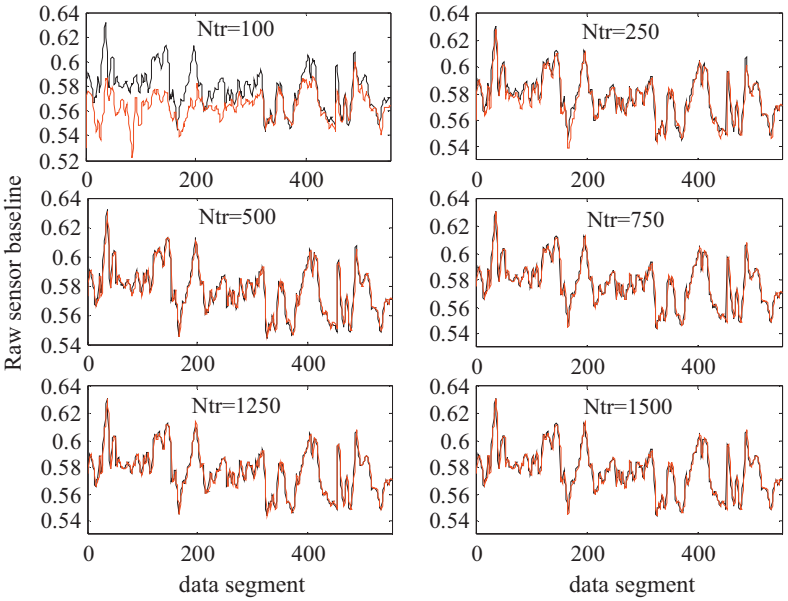

Fig. 11. TGS2620 sensor baseline predictions of the data segment in the Rectangular window.

where N denotes the length of test sequence **s** which is the true sequence, and $\hat{s}$ denotes the predicted output. In the ideal situation, if there is no error in prediction, then RMSEP = 0.

4. Results

4.1. Chaotic characteristic of long-term sensors data

Chaotic characteristic of long-term sensor response has been confirmed in this work. Through analysis of $\{x(n), n = 1,\ldots,N\}$ of each sensor, the time delays calculated by auto-correlated function method for TGS2620, TGS2201A and TGS2201B are 22, 24 and 23, respectively. The embedding dimension is calculated as $m = 3$. Three subfigures in Fig. 8 illustrate the three-dimensional $(x(t), x(t+\tau), x(t+2\tau))$ PSR plots of the extracted 13600 points for each sensor within a year which show the motion traces of sensors in PSR. Through the PSR plots in Fig. 8, we can find that the motion trace for each sensor has similar characteristic of chaotic attractor.

In addition, for further confirmation, the Lyapunov exponents λ_1, λ_2 and λ_3 of time series calculated using Wolf method are 0.1412, 0.2435, and 0.2933 for TGS2620, TGS2201A and TGS2201B sensor, respectively. The three Lyapunov exponents are positive, and thus there is obviously chaotic behavior in long-term sensor observation in terms of chaotic attractor theory. This promotes us to study the sensor drift in a novel chaotic time series method.

4.2. Sensor baseline and drift prediction

The phase space reconstruction and RBF neural network are used for raw sensor baseline and reconstructed drift prediction in this work. The long-term observation data for each sensor includes 13600 points (from September 04, 2011 to July 06, 2012.). To validate the long-term predictability of each sensor, the first 1000

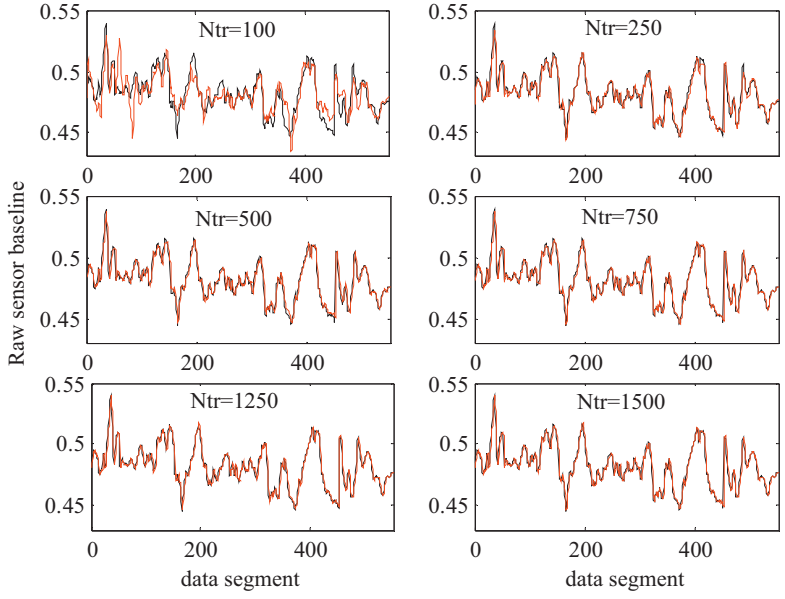

Fig. 12. TGS2201A sensor baseline predictions of the data segment in the Rectangular window.

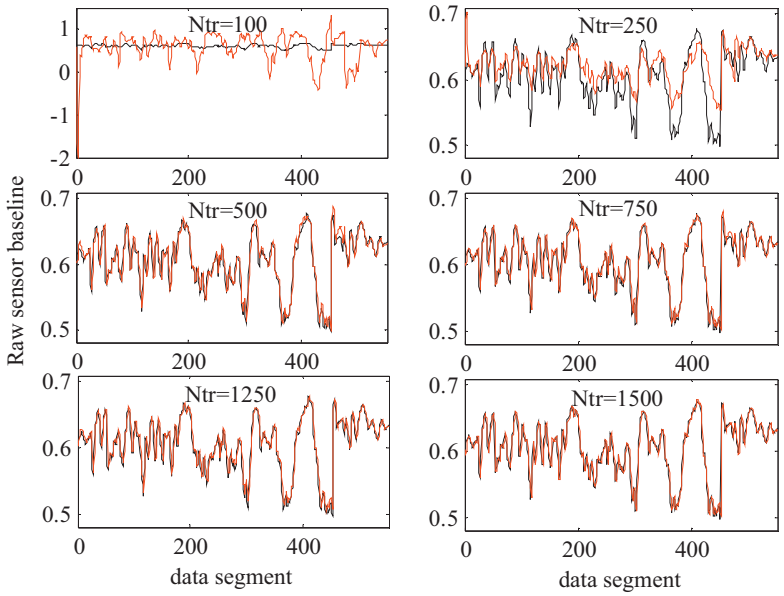

Fig. 13. TGS2201B sensor baseline predictions of the data segment in the Rectangular window.

points in September, 2011 (from September 04, 2011 to September 25, 2011) are used to train a prediction model. The remaining 12600 points (from September 26, 2011 to July 06, 2012) are used for model test. Fig. 9 presents the raw sensor baseline prediction results of three sensors. Fig. 9(a), (b) and (c) illustrate the predictions of TGS2620, TGS2201A and TGS2201B, respectively. For more clear visualization of the prediction, we show the prediction results of detailed local segment from 12000 to the end of the sequence in the Rectangular window (totally, 552 points) in Fig. 9(a), (b) and (c). The obvious results in Fig. 9(a'), (b') and (c') correspond to the three Rectangular windows of Fig. 9(a), (b) and (c), respectively. We can see in Fig. 9 that the long-term baseline prediction is successful.

Fig. 10 presents the prediction results of long-term drift signal reconstructed using DFT and IDFT. Similarly, Fig. 10(a), (b) and (c) illustrate reconstructed drift prediction of TGS2620, TGS2201A and TGS2201B, respectively. Fig. 10(a'), (b') and (c') correspond the local prediction of the three Rectangular windows from point 12000 to the end of the sequence in Fig. 10 (a), (b) and (c), respectively. Fig. 10 also demonstrates the effective drift prediction based on PSR and RBF neural network.

The prediction results shown in Figs. 9 and 10 are based on the RBF model trained by using the first 1000 data points of each sensor sequence. Due to that the number of training data points maybe useful to the potential researchers, we also experimentally show how many initial data points are required for prediction. Thus, the procedures of sensor baseline and drift predictions with smaller and larger numbers of training (Ntr) data points, such as 100, 250, 500, 750, 1250 and 1500, is performed, respectively. The predictions of TGS2620, TGS2201A and TGS2201B sensor baseline with different numbers (Ntr) of training data points are shown in Fig. 11, Fig. 12 and Fig. 13. From the three figures, we can find that the prediction performance can be approved when Ntr is equal to 500, and

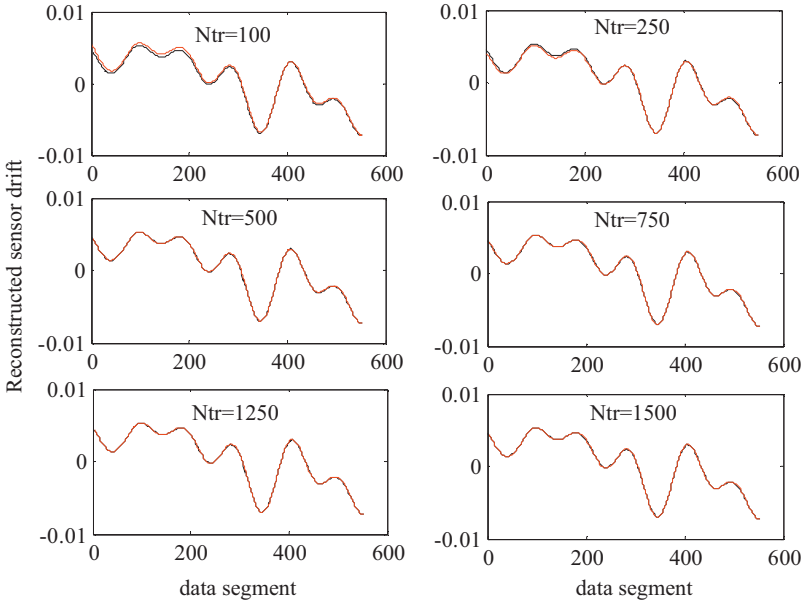

Fig. 14. TGS2620 sensor drift predictions of the data segment in the Rectangular window.

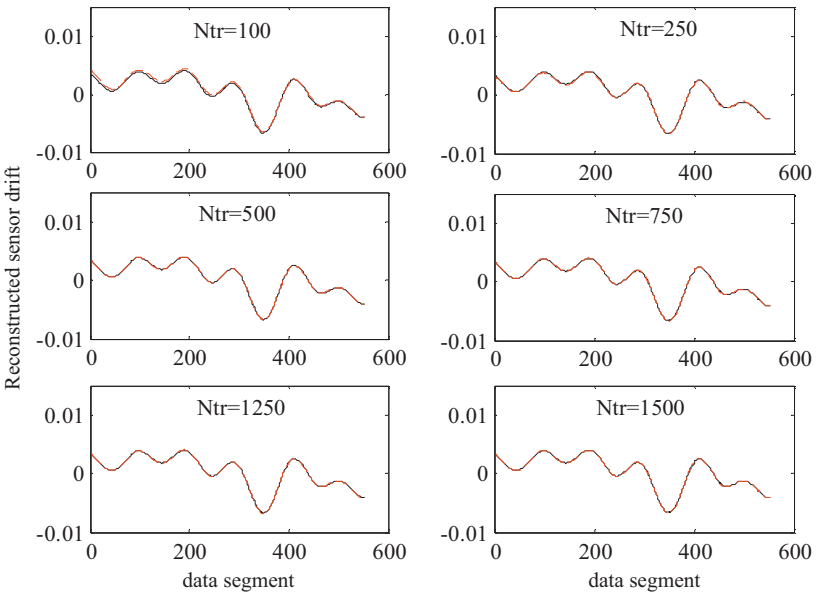

Fig. 15. TGS2201A sensor drift predictions of the data segment in the Rectangular window.

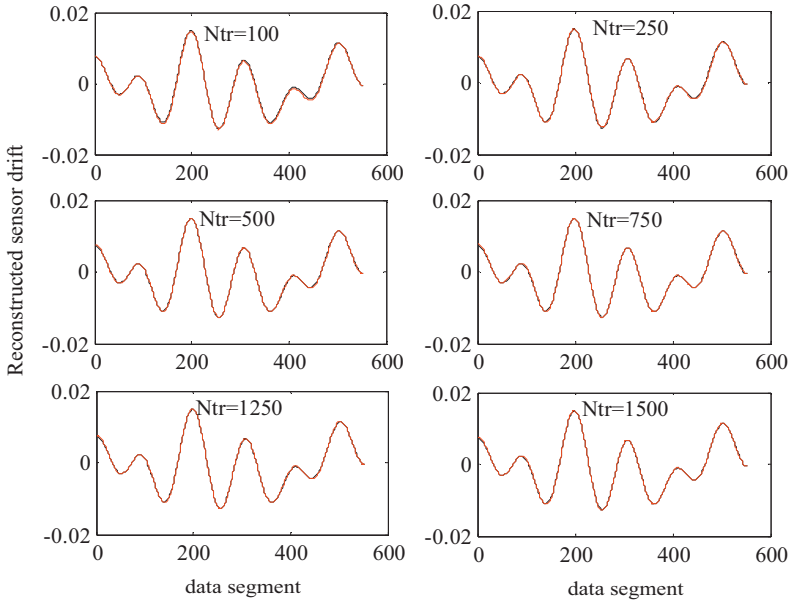

Fig. 16. TGS2201B sensor drift predictions of the data segment in the Rectangular window.

there is little change when the number Ntr of training data points is larger than 1000. In addition, we also present the sensor drift predictions of TGS2620, TGS2201A and TGS2201B with different numbers (Ntr) of training data points in Fig. 14, Fig. 15 and Fig. 16. We can also obtain from these figures that the smallest Ntr should be 500, and the modeling of RBF is enough when Ntr is not larger than 1000.

Besides the qualitative analysis, for quantitative evaluation of the prediction performance, Table 1 presents the RMSEPs of sensors' baseline and drift prediction modeling with different number of training data points calculated by using the Eq. (9). From Table 1, we can find that the RMSEP reduces with increasing number of Ntr, and an appropriate value of Ntr should be between 500 and 1000.

The results presented in this work confirm that long-term sensor baseline and drift signal has chaotic characteristic. Thus, it is difficult to find an effective drift compensation model in general ways. For example, the usual drift counteraction method is attributed to a fixed drift data set. However, the drift model constructed using the fixed data set may be not effective to a long-term drift. That is because the drift trend is uncertain, chaotic and unpredictable. Chaotic time series prediction is developed based on chaotic attractor in embedded phase space. PSR remains the properties of raw chaotic attractor, and the prediction is feasible in PSR of a chaotic time series.

5. Conclusions

This paper presents a novel methodology in treatment of chemical sensor drift in embedded phase space. The chaotic characteristic of long-term sensor time series is studied in terms of chaotic attractor theory and Lyapunov exponents. In view of the uncertainty, unpredictability and obvious chaotic characteristic, PSR and RBF neural network are combined together for long-term prediction of chaotic time series. In drift signal extraction, DFT technique is

used for spectrum analysis and drift frequency selection which excludes the environmental noise frequencies. IDFT is then used for time-domain drift signal reconstruction. Qualitative and quantitative results of sensor baseline and drift time series prediction demonstrate that the proposed chaos based model is effective in solutions of chemical sensor drift.

Acknowledgements

We would like to express our sincere appreciation to the anonymous reviewers for their insightful comments, which have greatly improved the quality of the paper.

This work was supported by the Key Science and Technology Research Programs (Nos. CSTC2010AB2002, CSTC2009BA2021). This work was also funded by New Academic Researcher Award for Doctoral Candidates granted by Ministry of Education in China.

References

[1] D. James, S.M. Scott, Z. Ali, W.T.O. Hare, Chemical sensors for electronic nose systems, Microchimica Acta 149 (2005) 1–17.
[2] S.M. Scott, D. James, Z. Ali, Data analysis for electronic nose systems, Microchimica Acta 156 (2007) 183–207.
[3] M. Holmberg, F.A.M. Davide, C. Di Natale, A.D. Amico, F. Winquist, I. Lundström, Drift counteraction in odour recognition applications: lifelong calibration method, Sensors and Actuators B 42 (1997) 185–194.
[4] A.C. Romain, J. Nicolas, Long term stability of metal oxide-based gas sensors for e-nose environmental applications: an overview, Sensors and Actuators B 146 (2010) 502–506.
[5] T. Artursson, T. Eklov, I. Lundström, P. Martensson, M. Sjostrom, M. Holmberg, Drift correction for gas sensors using multivariate methods, Journal of Chemometrics 14 (2000) 711–723.
[6] A. Ziyatdinov, S. Marco, A. Chaudry, K. Persaud, P. Caminal, A. Perera, Drift compensation of gas sensor array data by common principal component analysis, Sensors and Actuators B 146 (2010) 460–465.
[7] H. Ding, J. Liu, Z. Shen, Drift reduction of gas sensor by wavelet and principal component analysis, Sensors and Actuators B 96 (2003) 354–363.
[8] S. Di Carlo, M. Falasconi, E. Sanchez, A. Scionti, G. Squillero, A. Tonda, Increasing pattern recognition accuracy for chemical sensing by evolutionary based drift compensation, Pattern Recognition Letters 32 (2011) 1594–1603.
[9] M. Padilla, A. Perera, I. Montoliu, A. Chaudry, K. Persaud, S. Marco, Drift compensation of gas sensor array data by orthogonal signal correction, Chemometrics and Intelligent Laboratory Systems 100 (2010) 28–35.
[10] M.J. Wenzel, A.M. Brown, F. Josse, E.E. Yaz, Online drift compensation for chemical sensors using estimation theory, IEEE Sensors Journal 11 (1) (2011) 225–232.
[11] J. Zhang, K.C. Lam, W.J. Yan, H. Gao, Y. Li, Time series prediction using Lyapunov exponents in embedding phase space, Computers and Electrical Engineering 30 (2004) 1–15.
[12] M. Han, J. Xi, S. Xu, F.L. Yin, Prediction of chaotic time series based on the recurrent predictor neural network, IEEE Transactions on Signal Processing 52 (2004) 3409–3416.
[13] L. Zhang, F. Tian, C. Kadri, G. Pei, H. Li, L. Pan, Gases concentration estimation using heuristics and bio-inspired optimization models for experimental chemical electronic nose, Sensors and Actuators B Chemical 160 (2011) 760–770.
[14] L. Zhang, F. Tian, H. Nie, L. Dang, G. Li, Q. Ye, C. Kadri, Classification of multiple indoor air contaminants by an electronic nose and a hybrid support vector machine, Sensors and Actuators B Chemical 174 (2012) 114–125.
[15] L. Zhan, F. Tian, S. Liu, J. Guo, B. Hu, Q. Ye, L. Dang, X. Peng, C. Kadri, J. Feng, Chaos based neural network optimization for concentration estimation of indoor air contaminants by an electronic nose, Sensors and Actuators A Physical 189 (2013) 161–167.
[16] D. Huang, H. Leung, Reconstruction of drifting sensor responses based on papoulis-gerchberg method, IEEE Sensors Journal 9 (2009) 595–604.
[17] F. Taken, Detecting strange attractors in turbulence, in: Dynamical Systems and Turbulence, Springer, Berlin, 1980.
[18] H.D.I. Abarbanel, R. Brown, J.J. Sidorowich, L.S. Tsimring, The analysis of observed chaotic data in physical systems, Reviews of Modern Physics 65 (1993) 1331–1392.
[19] M.T. Rosenstein, J.J. Collins, C.J. De Luca, A practical method for calculating largest Lyapunov exponents from small data sets, Physica D: Nonlinear Phenomena 65 (1993) 117–134.
[20] L. Cao, Practical method for determining the minimum embedding dimension of a scalar time series, Physica D 110 (1997) 43–50.
[21] M. Lei, Z. Wang, Z. Feng, A method of embedding dimension estimation based on symplectic geometry, Physics Letters A 303 (1994) 179–189.
[22] M.T. Rosenstein, J.J. Collins, J. De Luca Carlo, Reconstruction expansion as a geometry based framework for choosing proper delay times, Physica D 73 (1994) 82–98.
[23] T. Buzug, G. Pfister, Optimal delay time and embedding dimension for delay time coordinates by analysis of the global and local dynamical behavior of strange attractors, Physical Review A 45 (1992) 7073–7084.
[24] A. Wolf, J.B. Swift, H.L. Swinney, J.A. Vastano, Determining Lyapunov exponents from a time series, Physica D: Nonlinear Phenomena 16 (1985) 285–317.
[25] E.N. Lorenz, Deterministic nonperiodic flow, Journal of the Atmospheric Sciences 20 (1963) 130–141.
[26] M. Casdagli, Nonlinear prediction of chaotic time series, Physica D 35 (1989) 335–356.
[27] Y. Lu, N. Sundararajan, P. Saratchandran, Performance evaluation of a sequential minimal radial basis function (RBF) neural network learning algorithm, IEEE Transactions on Neural Networks 9 (1998) 308–318.
[28] C. Jiann Long, I. Shafiqul, B. Pratim, Nonlinear dynamics of hourly ozone concentrations: nonparametric short term prediction, Atmospheric Environment 32 (1998) 1839–1848.

Biographies

Lei Zhang received his Bachelor degree in Electrical/Electronics engineering in 2009 from the Nanyang institute of technology, China; from September 2009 to December 2010, he studied for a MS degree in signal and information processing. He is presently with Chongqing University, pursuing his PhD degree in Circuits and Systems. His research interests include computational intelligence, artificial olfactory system, and nonlinear signal processing in Electronic Nose. He was honored by New Academic Researcher Award for Doctoral Candidates granted by Ministry of Education in China

Fengchun Tian received PhD degree in 1997 in electrical engineering from Chongqing University. He is currently a professor with the College of Communication Engineering of Chongqing University. His research interests include Electronic nose technology, artificial olfactory systems, pattern recognition, chemical sensors, signal/image processing, wavelet, and computational intelligence. In 2006 and 2007, he was recognized as a part-time Professor of GUELPH University, Canada.

Shouqiong Liu is now a senior engineer of Academy of Metrology And Quality Inspection, Chongqing. Her research interest was mainly analytical chemistry.

Lijun Dang received her Bachelor degree in School of Electronic and Information Engineering in 2011 from the Dalian University of Technology, China; from September 2011 to June 2012, she studied for a MS degree in circuits and system. Her research interests include circuits and system design in electronic nose technology.

Xiongwei Peng received his Bachelor degree in Communication Engineering in 2012 from the Chongqing University, China; from September 2012 to June 2015, he studied for a MS degree in circuits and system. His research interests include artificial neural network, genetic algorithms and optimizations.

Xin Yin received his Bachelor degree in Communication Engineering in 2012 from the Chongqing University, China; from September 2012 to June 2015, he studied for a MS degree in circuits and system. His research interests include electronic nose and circuit design.